Journal of Complex Networks (2024) **2**, Advance Access Publication on 26 February 2024
https://doi.org/10.1093/comnet/cnad052

Cross-diffusion induced instability on networks

Christian Kuehn[1,2,3] and Cinzia Soresina[4,5,†]

[1]*Department of Mathematics, Technical University of Munich, Boltzmannstr. 3, 85748 Garching bei München, Germany*

[2]*Munich Data Science Institute, Technical University of Munich, Walther-von-Dyck-Straße 10, 85748 Garching bei München, Germany*

[3]*Complexity Science Hub Vienna, Josefstädter Str. 39, 1080 Wien, Austria*

[4]*Department of Mathematics and Scientific Computing, University of Graz, Heinrichstr. 36, 8010 Graz, Austria*

[5]*Department of Mathematics, University of Trento, via Sommarive 14, 38123 Trento, Italy*

[†]Corresponding author. Email: cinzia.soresina@unitn.it

[Received on 3 August 2023; editorial decision on 14 December 2023; accepted on 27 December 2023]

The concept of Turing instability, namely that diffusion can destabilize the homogenous steady state, is well known either in the context of partial differential equations (PDEs) or in networks of dynamical systems. Recently, reaction–diffusion equations with non-linear cross-diffusion terms have been investigated, showing an analogous effect called cross-diffusion induced instability. In this article, we consider non-linear cross-diffusion effects on networks of dynamical systems, showing that also in this framework the spectrum of the graph Laplacian determines the instability appearance, as well as the spectrum of the Laplace operator in reaction–diffusion equations. We extend to network dynamics a particular network model for competing species, coming from the PDEs context, for which the non-linear cross-diffusion terms have been justified, e.g. via a fast-reaction limit. In particular, the influence of different topology structures on the cross-diffusion induced instability is highlighted, considering regular rings and lattices, and also small-world, Erdős–Réyni, and Barabási–Albert networks.

Keywords: Turing instability, cross-diffusion, dynamical networks, graph Laplacian, SKT model.

1. Introduction

A large number of real-life phenomena, for example in chemistry, ecology and biology, give rise to a rich variety of complex behaviours, including pattern formation. The spirals that originate from chemical reactions, fish skin and animal coat patterning, and spatial vegetation patterns result from a spontaneous drive for self-organization into regular structures, both in time and space. Mathematical principles that can drive the process of pattern formation have been established by Alan Turing in 1952. In his seminal article on the theory of morphogenesis [1], he discovered that patterns can arise as a result of the dynamical interplay between reaction and diffusion. This theory, known as Turing instability, provides a general and elegant explanation for the variety of patterns appearing in living systems: diffusion perturbs and destabilizes a homogeneous stable equilibrium, yielding to spatially inhomogeneous steady states.

On the other hand, Turing instability can also occur in networks of dynamical systems. In the seminal article by Othmer and Scriven [2], a general mathematical framework for the analysis of instabilities in networks has been proposed and applied to regular lattices or small networks. Later, it has been further explored and extended to more complex networks [3, 4], and even later to multiplex [5–7], time-varying [8] and stochastic [9] networks. Recently, Turing bifurcations have been investigated on one-dimensional

random ring networks where the probability of a connection between two nodes depends on the distance between them by using graphons [10]. The surprising finding is that the conditions leading to Turing instability are the same for both, the reaction–diffusion and the network systems, but while in the continuum case, we look at the eigenvalues of the Laplace operator, in the network case we need the spectrum of the graph Laplacian.

The graph Laplacian of an undirected network with N nodes is a real, symmetric and positive semi-definite matrix, whose elements are given by

$$l_{ij} = k_i\delta_{ij} - a_{ij}, \qquad i, j = 1, \dots, N, \tag{1.1}$$

where a_{ij} are the elements of the adjacency matrix and k_i is the degree of the node i, defined as

$$k_i = \sum_{i=1}^{N} a_{ij}, \quad i = 1, \dots, N, \qquad a_{ij} = \begin{cases} 1, & i \leftrightarrow j, \\ 0 & i \nleftrightarrow j, \end{cases} \quad i,j = 1, \dots, N.$$

In many areas and applications, it turns out that the eigenvalues of the graph Laplacian are useful tools, and for this reason, they have been intensively studied [11–16]. The eigenvalues Λ_α and eigenvectors $\underline{v}^{(\alpha)} = (v_1^{(\alpha)}, \dots, v_N^{(\alpha)})^\top$ of the graph Laplacian L are determined by

$$\sum_{j=1}^{N} l_{ij} v_j^{(\alpha)} = \Lambda_\alpha v_i^{(\alpha)}, \qquad i, \alpha = 1, \dots, N.$$

For an undirected network, eigenvalues are real and non-negative. It can be easily proven that 0 is an eigenvalue, $0 = \lambda_1 \leq \lambda_2 \leq \cdots \leq \lambda_N \leq N$, and that $\lambda_2 > 0$ if the network is connected. In particular, the eigenvalue λ_2 is often called *algebraic connectivity*, and it holds that

$$\lambda_2 \leq \frac{2|E|}{N-1},$$

where $|E|$ is the number of edges, and $2|E|$ can be obtained by summing the diagonal elements of the graph Laplacian. Properties of the spectrum have been investigated for particular network structures [17] including random graphs with given expected degrees [18] or more general random graphs [19]. Moreover, the spectrum of the graph Laplacian, as a quantity that encodes the topological structure of the underlying graph, also influences the dynamical properties, such as the stability of the synchronous state, which has been investigated for quite some time [20, 21] and has more recently been referred to as master stability function approach [22–25].

The diffusion on the network given by the graph Laplacian only is a linear diffusion and considers pairwise interactions. More recently, non-linear diffusion (also called non-linear coupling or, in ecology, *non-linear dispersal*), and higher-order interactions on networks have been proposed and investigated, see for instance [26–29].

It is widely accepted that the Turing instability is induced by diffusion and requires an activator–inhibitor scheme of interaction between agents [30]. However, in the context of continuous space reaction–diffusion systems a cross-diffusion model has been proposed (and later justified, e.g. via a fast-reaction limit) to describe the spatial segregation of the species [31]. In this model, also known as Shigesada–Kawasaki–Teramoto (SKT) system, the reaction part does not generate an activator–inhibitor mechanism, but spatial patterns may arise thanks to cross-diffusion terms. These terms model those

situations in which the movements of individuals of a species depend not only on the species itself but also on the presence of other species. This mechanism can also be observed in other contexts: for instance in the presence of chemotaxis, or also in epidemiology, where the movements of susceptible individuals are clearly influenced by the presence of infected ones [32]. Then, cross-diffusion can destabilize a homogeneous equilibrium and induce pattern formation, even when it is not possible via standard diffusion terms; this phenomenon is known as cross-diffusion-induced instability. Reaction–cross-diffusion models have been extensively studied from different points of view and related to several applications (see [33–40] and references therein).

Knowing all these ingredients, we are interested in the extension and the study of non-linear cross-diffusion and cross-diffusion-induced instability on complex networks. In addition to the natural pairing between continuous and discrete space models, this extension has been naively inspired by the discretization of reaction–cross-diffusion equations using finite differences [41]. In fact, the (regular) mesh can be viewed as a regular lattice. Moreover, a natural question at this point is *when/if* the discretized systems show the same patterns as the continuous model (depending on the number of mesh points).

The theory of pattern formation on networks has been developed for several network structures and dynamical rules, and several works have also investigated cross-diffusion terms (or coupling) [42–44], where, however, the cross-diffusion terms considered are relatively simple (linear). We show that the theory of pattern formation on networks still holds considering general non-linear cross-diffusion terms (written in terms of the graph Laplacian). Also in this case, the conditions for cross-diffusion-driven instability are the same for the network and the continuous space case, where the eigenvalues of the graph Laplacian play the role of the eigenvalue of the Laplace operator. Then, we propose and investigate the SKT cross-diffusion model for competing species on a network. The model generalizes the model investigated in [45] including only standard diffusive coupling, which is known to have no heterogeneous (positive) steady states in the weak competition regime. As in the continuous setting, cross-diffusion is the key ingredient in producing stable patterns, i.e. non-homogeneous (on the nodes of the network) steady-state solutions. Our attention is however focused on the network structures (from regular rings, two-dimensional-lattices to different complex/random graphs) in order to show, how they influence the possible dynamics of the system. In particular, we look at the spectrum of the graph Laplacian (or its distribution for random graphs). The aim of this work is mainly to point out that non-linear cross-diffusion terms can be useful ingredients in the study of complex systems, and that they can give rise to very rich dynamics depending crucially on the network topology.

The article is organized as follows. In Section 2, we establish the general framework for cross-diffusion systems on networks, and we extend the Turing instability analysis to cross-diffusion-induced instability. In Section 3, we propose a cross-diffusion model for competing species, inspired by the discretization of the SKT model on a one-dimensional domain. This model is analysed on different network structures, from regular rings and lattices, to more complex networks. The non-homogeneous steady states are studied, and the distributions of the eigenvalues for different network structures are presented. The focus of this section is to understand if particular structures are more favourable to leading to cross-diffusion-induced instability. Finally, in Section 4 some concluding remarks can be found. The formal fast-reaction limit leading to the non-linear cross-diffusion terms in the SKT model on networks is presented in Appendix A. The Python scripts for the simulations are freely accessible in the GitHub folder [46].

2. The general framework

In this section, we extend the Turing instability analysis on networks to cross-diffusion systems. This type of system can model complex natural phenomena in which non-trivial and non-linear effects also affect the diffusion of the involved quantities. For instance, in ecology, competition of species can cause

migrations as a prey species tries to avoid predators, while in epidemiology susceptible individuals may try to avoid infected ones.

We consider an undirected network of N nodes. The network topology is encoded in the graph Laplacian $L \in \mathbb{R}^{N\times N}$. On each node, we consider two state variables $(\phi_i, \psi_i) = (\phi_i(t), \psi_i(t))$, evolving over time. The dynamics on each node is influenced by different components:

- the single node dynamics, described by the functions $f,\ g$,
- standard coupling (random movements), expressed as a diffusive flux of a species to other nodes in terms of potential difference. The coupling parameters, also called diffusion coefficients, are denoted by $D_i,\ i = 1, 2$.
- non-linear cross-diffusion effects, modelling the influence on the coupling of one state variable due to the other one. For instance, in ecology, the presence of a species may increase the diffusion of others. The cross-diffusion coefficients are denoted by $D_{ij},\ i,j = 1, 2$, while non-constant functions $c_i,\ i = 1, 2$ describe the type of interaction.
- self-diffusion effects, due to the presence of the same state variable. The self-diffusion coefficients are denoted by $D_{ii},\ i = 1, 2$, while non-constant functions $s_i,\ i = 1, 2$ describe the type of interaction.

All the considered functions are supposed to be regular enough (at least sufficiently smooth). Then, the network dynamics can be modelled by

$$\begin{cases} \dot{\phi}_i = f(\phi_i, \psi_i) - D_1 \sum_{j=1}^{N} l_{ij}\phi_j - D_{11} \sum_{j=1}^{N} l_{ij} s_1(\phi_j)\phi_j - D_{12} \sum_{j=1}^{N} l_{ij} c_1(\psi_j)\phi_j, \\ \dot{\psi}_i = g(\phi_i, \psi_i) - D_2 \sum_{j=1}^{N} l_{ij}\psi_j - D_{22} \sum_{j=1}^{N} l_{ij} s_2(\psi_j)\psi_j - D_{21} \sum_{j=1}^{N} l_{ij} c_2(\phi_j)\psi_j, \\ i = 1, \dots, N, \end{cases} \tag{2.1}$$

where the overdot denotes time differentiation, and l_{ij} are the elements of the graph Laplacian L as defined in equation (1.1) and they appear in the diffusion terms (standard, cross- and self-diffusion) since they encode the network structure.

As usual in Turing instability analysis, we consider a stable steady state for the single node dynamics (ϕ_*, ψ_*), such that

$$f(\phi_*, \psi_*) = g(\phi_*, \psi_*) = 0, \quad \operatorname{tr}(J_*) < 0, \quad \det(J_*) > 0,$$

where the matrix J_* is the Jacobian of the single node dynamics evaluated at the homogeneous steady state

$$J_* = \begin{pmatrix} f_\phi(\phi_*, \psi_*) & f_\psi(\phi_*, \psi_*) \\ g_\phi(\phi_*, \psi_*) & g_\psi(\phi_*, \psi_*) \end{pmatrix}.$$

It turns out that the state $(\underline{\phi}_*, \underline{\psi}_*)$, where

$$\phi_i = \phi_*, \quad \psi_i = \psi_*, \quad i = 1, \dots, N, \tag{2.2}$$

is a homogeneous (on the nodes of the network) steady state for the network. Cross-diffusion induced instability arises when (ϕ_*, ψ_*) becomes unstable to inhomogeneous perturbations thanks to cross-diffusion terms.

We now want to find conditions for the destabilization of the homogeneous steady-state.

PROPOSITION 2.1 Consider system (2.1) and the homogeneous steady state $(\underline{\phi}_*, \underline{\psi}_*)$ defined in (2.2). Consider the characteristic matrix associated to the eigenvalues Λ_α of the graph Laplacian

$$M_\alpha^* = J^* - \Lambda_\alpha D_*, \qquad \alpha = 1, \dots, N$$

where the matrix J_* is Jacobian of the single node dynamics evaluated at the steady state and the matrix D_* is the linearization of the diffusion part evaluated at the steady state, given by

$$D_* = \begin{pmatrix} D_1 + D_{11}\left(s_1(\phi_*) + s_1'(\phi_*)\phi_*\right) + D_{12}c_1(\psi_*) & D_{12}c_1'(\psi_*)\phi_* \\ D_{21}c_2'(\phi_*)\psi_* & D_2 + D_{22}\left(s_2(\psi_*) + s_2'(\psi_*)\psi_*\right) + D_{21}c_2(\phi_*) \end{pmatrix}.$$

Then, in order to destabilize the homogeneous steady state, the characteristic matrix M_α^* must have a positive eigenvalue for at least one α corresponding to one eigenvalue Λ_α of the graph Laplacian.

Proof. The linear stability analysis is effectively a suitable combination of the standard cases on networks and in continuous media. We introduce small perturbations $\delta\phi_i$, $\delta\psi_i$ to the homogeneous state as

$$(\phi_i, \psi_i) = (\phi_*, \psi_*) + (\delta\phi_i, \delta\psi_i), \qquad i = 1, \dots, N,$$

and substitute this into equation (2.1). Linearized differential equations for $\delta\phi_i$, $\delta\psi_i$ are

$$\begin{cases} \dot{\delta\phi}_i = f_\phi(\phi_*, \psi_*)\delta\phi_i + f_\psi(\phi_*, \psi_*)\delta\psi_i - D_1\sum_{j=1}^N l_{ij}\delta\phi_j \\ \qquad -D_{11}\sum_{j=1}^N l_{ij}\left(s_1(\phi_*) + s_1'(\phi_*)\phi_*\right)\delta\phi_j - D_{12}\sum_{j=1}^N l_{ij}\left(c_1(\psi_*)\delta\phi_j + c_1'(\psi_*)\phi_*\delta\psi_j\right), \\ \dot{\delta\psi}_i = g_\phi(\phi_*, \psi_*)\delta\phi_i + g_\psi(\phi_*, \psi_*)\delta\psi_i - D_2\sum_{j=1}^N l_{ij}\delta\psi_j \\ \qquad -D_{22}\sum_{j=1}^N l_{ij}\left(s_2(\psi_*) + s_2'(\psi_*)\psi_*\right)\delta\psi_j - D_{21}\sum_{j=1}^N l_{ij}\left(c_2'(\phi_*)\psi_*\delta\phi_j + c_2(\phi_*)\delta\psi_j\right), \\ i = 1, \dots, N, \end{cases}$$

and they can be written as

$$\begin{pmatrix} \dot{\delta\phi}_i \\ \dot{\delta\psi}_i \end{pmatrix} = J_* \begin{pmatrix} \delta\phi_i \\ \delta\psi_i \end{pmatrix} - D_* \sum_{j=1}^N l_{ij} \begin{pmatrix} \delta\phi_j \\ \delta\psi_j \end{pmatrix}, \quad i = 1, \dots, N. \tag{2.3}$$

We consider the spectrum of the graph Laplacian

$$\sum_{j=1}^{N} l_{ij} v_j^{(\alpha)} = \Lambda_\alpha v_i^{(\alpha)}, \quad i, \alpha = 1, \dots, N,$$

where Λ_α and $v^{(\alpha)}$ represent the eigenvalues and their associated eigenvectors, respectively. By expanding the perturbations $\delta\phi_i$, $\delta\psi_i$ over the set of Laplacian eigenvectors $v_i^{(\alpha)}$ as

$$\delta\phi_i(t) = \sum_{\alpha=1}^{N} \gamma_\alpha e^{\lambda_\alpha t} v_i^{(\alpha)}, \qquad \delta\psi_i(t) = \sum_{\alpha=1}^{N} \beta_\alpha e^{\lambda_\alpha t} v_i^{(\alpha)}, \qquad i, \alpha = 1, \dots, N.$$

where the constants γ_α and β_α refer to the initial conditions, system (2.3) is transformed into N independent linear equations for different normal modes, resulting in the following eigenvalue equation for each α:

$$\lambda_\alpha \begin{pmatrix} \gamma_\alpha \\ \beta_\alpha \end{pmatrix} = (J^* - \Lambda_\alpha D_*) \begin{pmatrix} \gamma_\alpha \\ \beta_\alpha \end{pmatrix} = M_\alpha^* \begin{pmatrix} \gamma_\alpha \\ \beta_\alpha \end{pmatrix}, \qquad \alpha = 1, \dots, N,$$

where the matrix

$$M_\alpha^* = J^* - \Lambda_\alpha D_*, \qquad \alpha = 1, \dots, N$$

is the characteristic matrix associated to the eigenvalues Λ_α of the graph Laplacian. Then, in order to destabilize the homogeneous steady state, the characteristic matrix M_α^* must have a positive eigenvalue for at least one α corresponding to one eigenvalue Λ_α of the graph Laplacian, since the mode associated to this eigenvalue is then unstable. Note that the eigenvalues of the graph Laplacian appear only in combination with diffusion coefficients. □

Remark. Since the eigenvalues of the graph Laplacian are non-negative, the expression of the characteristic matrix M_α^* turns out to be the same as in the PDEs setting, and the eigenvalues of the graph Laplacian play the role of the eigenvalues of the Laplace operator. Then, the conditions on the parameters leading to the instability of the homogeneous steady state are the same.

In summary, the Turing instability analysis in the continuous setting and on discrete models can be adapted to cross-diffusion systems on networks. Note that depending on the single node dynamics, it is not always possible to destabilize the homogeneous equilibrium by means of standard diffusion terms only (in particular when the single node dynamics does not have the activator–inhibitor structure). Cross-diffusion induced instability appears when the homogeneous steady state becomes unstable to inhomogeneous perturbations, due to the additional presence of cross-diffusion terms.

Remark. When $\Lambda_\alpha = 0$ the characteristic matrix (3.4) reduces to the Jacobian J_* of the single node dynamics evaluated at the coexistence steady state. Therefore, the zero-eigenvalue provides information about the dynamics of an isolated node. The non-zero eigenvalues instead account for the more complex behaviour of the network.

3. The SKT model on networks

The goal of this section is to show a particular case in which the non-linear cross-diffusion term destabilizes the homogeneous equilibrium state leading to non-trivial steady states and to study the role and the influence of the network topology on these states. To achieve this, we present here a cross-diffusion model on networks for competing species, analogous to the SKT model presented in the framework of PDEs (see [33, 37] and references therein).

We consider two species, u and v, competing for the same resource. A system of ODEs describes the dynamics of an isolated node

$$\begin{cases} \dot{u} = f(u,v) = r_1 u - a_1 u^2 - b_1 uv, \\ \dot{v} = g(u,v) = r_2 v - b_2 uv - a_2 v^2, \end{cases} \tag{3.1}$$

where r_1, r_2 are the growth rates, a_1, a_2 the intra-specific competition rates and b_1, b_2 the inter-specific competition rates. It is simple to show that the outcomes of (3.1) can be the total extinction, competitive exclusion or the coexistence of the species, depending on the parameter values and on the initial conditions. The system admits a coexistence equilibrium (u_*, v_*) which is stable in the weak competition regime ($a_1a_2 - b_1b_2 > 0$) and unstable in the strong competition regime ($a_1a_2 - b_1b_2 > 0$), when it exists.

We consider now a network of N nodes, its topology being fixed by the Laplacian matrix of the graph $L = (l_{ij})_{i,j=1,\dots,N}$. On each node the population sizes are denoted with u_i, v_i, $i = 1, \dots, N$ and the dynamics on each node in case of isolation (neglecting the diffusion process) is given by (3.1). When the nodes are connected in a network, we consider diffusive movements of the individuals between linked nodes modelled in the usual way

$$-\sum_{j=1}^{N} l_{ij} u_j = \sum_{j=1}^{N} (u_j - u_i), \qquad i = 1, \dots, N.$$

Then, we consider cross- and self-diffusion effects, which cause extra movements of individuals due to intra- and inter-competition pressure. In particular, individuals living on a node leave to reach other nodes because of the presence of individuals of the same species (self-diffusion) or of the competing species (cross-diffusion).

In detail, they can be described by

$$-\sum_{j=1}^{N} l_{ij} u_j^2, \qquad -\sum_{j=1}^{N} l_{ij} v_j u_j, \qquad i = 1, \dots, N.$$

Remark. This particular form can be justified by a mechanistic derivation exploiting processes happening at different time scales, similar to the SKT model in the PDEs context. The formal derivation can be found in the Appendix.

Then, the system of ODEs describing the dynamics of the network is given by

$$\begin{cases} \dot{u}_i = f(u_i, v_i) - d_1 \sum_{j=1}^{N} l_{ij} u_j - D_{11} \sum_{j=1}^{N} l_{ij} u_j^2 - D_{12} \sum_{j=1}^{N} l_{ij} v_j u_j, \\ \dot{v}_i = g(u_i, v_i) - d_2 \sum_{j=1}^{N} l_{ij} v_j - D_{22} \sum_{j=1}^{N} l_{ij} v_j^2 - D_{21} \sum_{j=1}^{N} l_{ij} u_j v_j, \\ i = 1, \dots, N \end{cases} \tag{3.2}$$

where d_i, D_{ij}, $i,j = 1,2$ are the coupling strengths (or diffusion coefficients).

In order to investigate cross-diffusion instability effects, it is sufficient to consider $D_{11} = D_{22} = 0$ and $d_1 = d_2 = d$ (analogous to the PDEs case). This choice corresponds to the simpler cross-diffusion system

$$\begin{cases} \dot{u}_i = f(u_i, v_i) - d \sum_{j=1}^{N} l_{ij} u_j - D_{12} \sum_{j=1}^{N} l_{ij} v_j u_j, \\ \dot{v}_i = g(u_i, v_i) - d \sum_{j=1}^{N} l_{ij} v_j - D_{21} \sum_{j=1}^{N} l_{ij} u_j v_j. \\ i = 1, \dots, N. \end{cases} \tag{3.3}$$

Following [45], it can be proven that the solutions to (3.3) with non-negative initial conditions remain non-negative all the time. Here, we use the notation $x \leq y$ with $x, y \in \mathbb{R}^N$ to indicate that $x_i \leq y_i \, \forall i \in \{1, \dots, n\}$.

THEOREM 3.1 If $\underline{u}, \underline{v} : \mathbb{R}_+ \to \mathbb{R}^N$ satisfy (3.3) and $\underline{u}(0), \underline{v}(0) \geq 0$, then $\underline{u}(t), \underline{v}(t) \geq 0$ for all $t > 0$.

Proof. We must prove the fact that the set

$$S = \{(u^1, v^1) \in \mathbb{R}^N \times \mathbb{R}^N : u^1 \geq 0, \, v^1 \geq 0\}$$

is a positively invariant region for system (3.3). The calculations follow the proof in [45] for the system with only standard coupling. Due to cross-diffusion, we have extra terms, but it is easy to see that they have the correct sign configuration. □

Remark. When only linear diffusion is considered, *a priori* bounds for the solutions can be obtained. With cross-diffusion terms, we cannot obtain comparison results as in [45, Theorem 3.2].

3.1 *Cross-diffusion induced instability in the SKT model on networks*

We now want to find conditions for the destabilization of the homogeneous steady state.

PROPOSITION 3.2 Consider system (3.3) with the single node dynamics given in equation (3.1) in the weak competition regime (namely $a_1 a_2 - b_1 b_2 > 0$). Consider the quantities α and β defined as in [33]

$$\alpha := (b_2 u_* - a_2 v_*) v_*, \quad \beta := (b_1 v_* - a_1 u_*) u_*,$$

and parameter d as bifurcation parameter. Then,

- if $D_{12}\alpha + D_{21}\beta \leq 0$, then no bifurcation points can appear, independently of the network topology.
- if $D_{12}\alpha + D_{21}\beta > 0$, a bifurcation point can appear depending on the eigenvalues of the Laplacian of the graph. In detail, we obtain the following threshold

$$\Lambda > \Lambda_* = \frac{\det(J_*)}{D_{12}\alpha + D_{21}\beta}.$$

Proof. We proceed with the linearized analysis close to the homogeneous steady state in which $u_i = u_*,\ v_i = v_*,\ i = 1,\dots,N$ in the weak-competition regime. Then, according to Section 2, the characteristic matrix associated to an eigenvalue Λ of the graph Laplacian is

$$M_\Lambda = J_* - \Lambda D_* = \begin{pmatrix} -a_1 u_* & -b_1 u_* \\ -b_2 v_* & -a_2 v_* \end{pmatrix} - \Lambda \begin{pmatrix} d + D_{12} v_* & D_{12} u_* \\ D_{21} v_* & d + D_{21} u_* \end{pmatrix}. \tag{3.4}$$

Since in the weak competition case $\mathrm{tr}(J_*) < 0$ and $\det(J_*) > 0$ and, remembering that the graph Laplacian has non-negative eigenvalues, then the characteristic matrix has a negative trace and its determinant determines the stability/instability of the homogeneous steady state. Then, a cross-diffusion induced instability may appear if its determinant becomes negative for at least one Λ, since the mode associated to this eigenvalue is then unstable. Taking d as the bifurcation parameter, the determinant can be written as

$$\det(M_\Lambda) = A_\Lambda d^2 + B_\Lambda d + C_\Lambda, \tag{3.5}$$

where the coefficients $A_\Lambda,\ B_\Lambda,\ C_\Lambda$ of the second-order polynomial in d are given by

$$A_\Lambda = \Lambda^2, \quad B_\Lambda = D_{12} v_* \Lambda^2 + D_{21} u_* \Lambda^2 - \mathrm{tr}(J_*)\Lambda, \quad C_\Lambda = -(D_{12}\alpha + D_{21}\beta)\Lambda + \det(J_*).$$

In order to have a negative determinant, we need $C_\Lambda < 0$. Note that there are two cases:

- if $D_{12}\alpha + D_{21}\beta \leq 0$, then $C_\Lambda < 0$ independently on Λ. Therefore, no bifurcations can appear, independently of the network topology.
- if $D_{12}\alpha + D_{21}\beta > 0$, then C_Λ can be negative for a sufficient large Λ. Therefore, bifurcations can appear depending on Λ the eigenvalues of the Laplacian of the graph. In detail, the condition $C_\Lambda < 0$ gives the following threshold

$$\Lambda > \Lambda_* = \frac{\det(J_*)}{D_{12}\alpha + D_{21}\beta}.$$

□

Remark. This condition can be combined with other information on the spectrum of a particular graph to prove the stability of the homogeneous state. Since $\Lambda_N \leq N$, the simplest observation is that if $N < \Lambda_*$, then no cross-diffusion induced instability is possible. We can also obtain conditions regarding the stability of a particular mode (eigenvalue). For instance, for a regular graph of N nodes and degree $2K$, we know that the first non-trivial eigenvalue (also known as *algebraic connectivity*) satisfies $\Lambda_2 \leq 2KN/(N-1)$. If $\Lambda_* > 2KN/(N-1)$, then the mode related to Λ_2 is stable.

Remark. From equation (3.5), it is easy to see the cross-diffusion terms are the key ingredient to the appearance of non-homogeneous steady states. In fact, if $D_{12} = D_{21} = 0$, then $\det(M_\Lambda) > 0$. This means that, regardless of the network structure, standard diffusion terms cannot lead to Turing instability.

To characterize the instability region and the bifurcation points, we now look at the determinant of the characteristic matrix as a second-order polynomial in Λ, namely

$$\det(M_\Lambda(\Lambda)) = A_d\Lambda^2 - B_d\Lambda + C_d,$$

where

$$A_d = d(d + D_{12}v_* + D_{21}u_*), \quad B_d = (D_{12}\alpha + D_{21}\beta + d\,\mathrm{tr}(J_*)), \quad C_d = \det J_*.$$

The instability region corresponds to the values of Λ for which $\det(M_\Lambda)$ is negative. Since $\det(M_\Lambda)$ is a second-order polynomial in Λ, provided that its discriminant is positive, we can obtain an instability region $\Omega_* = (\Lambda_{*1}, \Lambda_{*2})$ for the eigenvalues of the graph Laplacian. In detail,

$$\Lambda_{*1,*2} = \frac{B_d \mp \sqrt{B_d^2 - 4A_dC_d}}{2A_d}, \quad \text{provided that } B_d^2 - 4A_dC_d > 0. \tag{3.6}$$

3.2 *Cross-diffusion induced instability and graph topology*

This section is devoted to showing, how the obtained conditions and thresholds combine with the network topology and what kind of non-homogeneous steady states arises thanks to cross-diffusion induced instability. To this end, we use simple network topologies, in order to highlight the effect per see, but also other different types of graphs, including random graphs such as *small world* and *Erdős–Rényi* networks. The different network structures have been generated using the Python [47] package NetworkX [48]. The same parameter set describes the dynamics, but different outcomes emerge as the result of the underlying topology. As a key factor, the spectral properties of the graph Laplacian are compared.

The parameter values used in the simulations are

$$r_1 = 5,\ r_2 = 2,\ a_1 = 3,\ a_2 = 3,\ b_1 = 1,\ b_2 = 1,\ d = 0.03,\ d_{12} = 3,\ d_{21} = 0, \tag{3.7}$$

and correspond to the weak competition case ($a_1a_2 - b_1b_2 > 0$), namely the homogeneous steady state is stable for the single node dynamics. The remaining parameters related to the network structure will be specified each time in the text.

Remark. In the simulations, we do not vary the linear diffusion parameter d. As in the PDEs case, large values of d tend to stabilize the homogeneous state.

3.2.1 *Regular ring lattice* A $2K$-regular ring lattice is a graph with N nodes in a ring structure in which each node is connected to its $2K$ neighbours (K on either side) [49]. The associated graph Laplacian is a matrix with three bands (in the centre and in the corners NE and SW), defined by

$$l_{ij} = \begin{cases} 2K, & i = j, \\ -1, & 0 < \min\{(i-j) \bmod N, (j-i) \bmod N\} \le K, \\ 0, & \text{otherwise.} \end{cases}$$

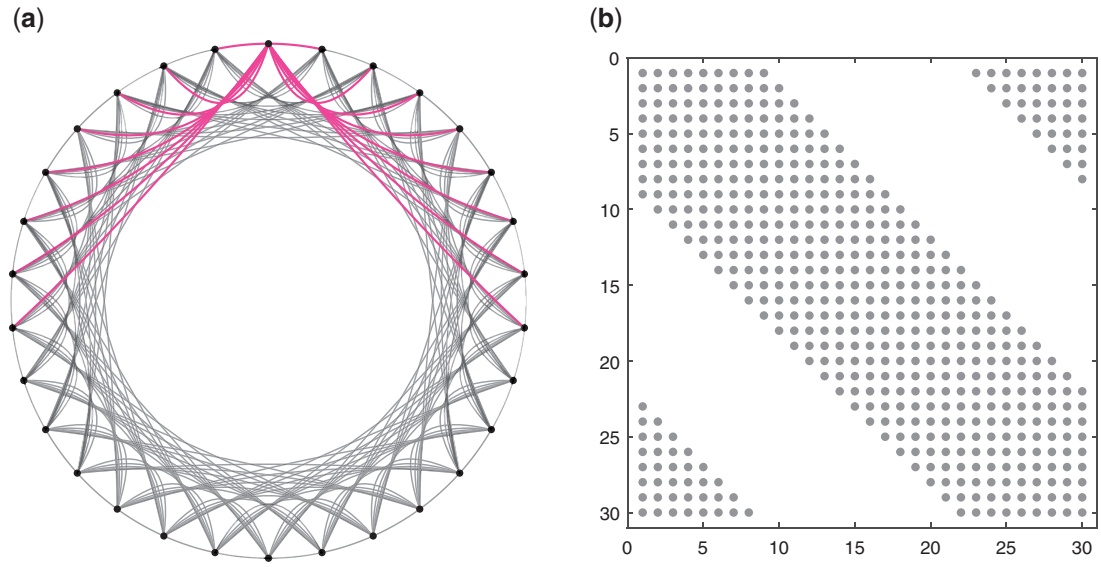

FIG. 1. Structure of a $2K$-regular ring lattice and of its graph Laplacian. (a) Structure of the regular $2K$-ring with $N = 30$, $K = 8$, in which the $2K$ nearest neighbours (K on each side) of a particular node are highlighted in magenta. (b) Structure of the corresponding graph Laplacian, where grey dots indicate non-zero elements. For interpretation of the color references, the reader is referred to the web version of this article.

The structure of the network and of the graph Laplacian are shown in Fig. 1. The closed formula for the eigenvalues is

$$\Lambda_j = 2K - \sum_{k=1}^{K} 2\cos\left(\frac{2\pi k(j-1)}{N}\right), \quad j = 1, \dots, N.$$

In Fig. 2, the spectrum of the graph Laplacian is reported for different values of N and K, in order to study the possible appearance of patterns. The instability region $\Omega_* = (\Lambda_{*1}, \Lambda_{*2})$, given in (3.6), is marked with a red stripe. If at least one eigenvalue of the graph Laplacian is located in the instability region Ω_*, then the corresponding modes are destabilized, the trivial state becomes unstable and system (3.3) admits a stable non-homogeneous steady state.

We can observe in Fig. 2a that the value of non-zero eigenvalues increases when K increases (and N is fixed); for small values of K the spectrum lies below the threshold value Λ_{*1} while increasing K we pass from a situation in which part of the spectrum is located in the instability region to a situation in which only the smallest non-zero eigenvalue is present. Finally, for $K > 25$ all the non-zero eigenvalues are greater than the threshold value Λ_{*2}, namely no stable pattern can appear. On the contrary, increasing N with a fixed K leads to smaller eigenvalues in the spectrum intersecting the instability region (Fig. 2b). However, this will lead to different non-homogeneous solutions.

In Fig. 3, we show different stable steady states of the cross-diffusion model (3.3) for the ring structure of $N = 100$ nodes and four different values of K, corresponding to different locations of the spectrum with respect to the instability region (Fig. 2a). In particular, the dots mark the values of the variables u_i or v_i at the stable configuration. With $K = 3$, the stable configuration is not homogeneous (namely the nodes

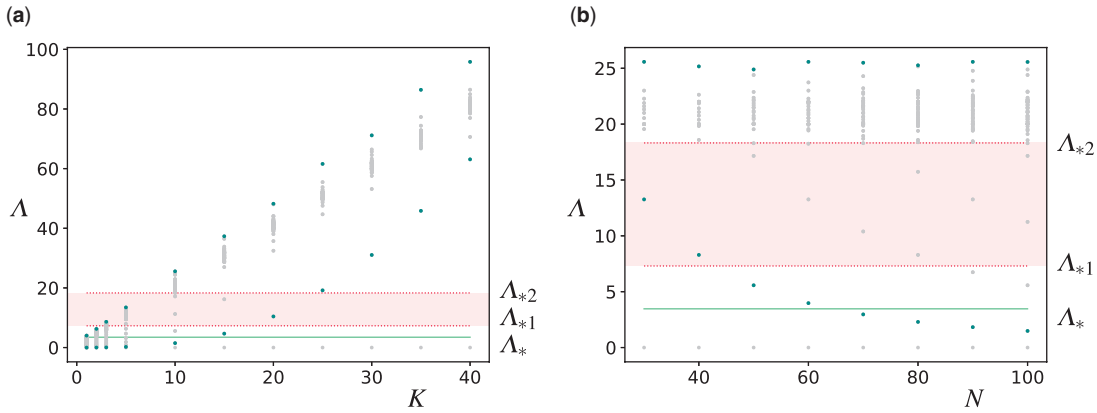

FIG. 2. Cross-diffusion driven instability on $2K$-regular rings for different values of K and $N = 100$ (a) and different values of N and $K = 10$ (b). Grey dots mark the eigenvalues of the Graph Laplacian, while green dots highlight the smallest and the largest non-zero eigenvalues. Horizontal lines denote the values Λ_{*1}, Λ_{*2} from equation (3.6) (red dotted) and Λ_* (green solid), and the instability region $\Omega_* = (\Lambda_{*1}, \Lambda_{*2})$ is marked with the red stripe (values relevant to the parameter set in equation (3.7)). For interpretation of the color references, the reader is referred to the web version of this article.

do not reach the steady state (u_*, v_*) but different values). With higher K different stable configurations can appear, showing a pattern on the network.

3.2.2 *Two-dimensional lattices* We consider here three different two-dimensional grid graphs: triangular, square and hexagonal lattices, sketched in Fig. 4. Note that, except for 'boundary nodes', each node in the lattice has the same degree: 6 in the triangular lattice, 4 in the square lattice and 3 in the hexagonal lattice.

In Fig. 4, we show the location of the spectra of the three topologies ($N = 110$) with respect to the instability region (obtained using the parameter set in equation (3.7)). Note that the value of the largest eigenvalue does not change significantly increasing N, since the lattices are almost regular. It can be observed that non-homogeneous steady states cannot appear on the hexagonal grid, while in the triangular and square lattices, the homogeneous steady state is unstable. The steady patterns on a triangular and square lattice with $N = 400$ nodes are shown in Fig. 5 with respect to the u variable. In this figure, different colours denote different values of the state variable u and each node in the networks is coloured accordingly to the final steady state. The parameter set is the same for both network structures but the final steady states are different: on the square lattice (Fig. 4b) we clearly see an alternation of nodes with higher population and nodes with lower population, contrary to what we observe on a triangular lattice (Fig. 4a).

3.2.3 *Random graphs* We now turn our attention to several random graphs. Also in this case, we want to study the influence of a particular structure on the emergence of stable patterns in the network. As in the previous section, we look at the non-zero eigenvalues of the graph Laplacian. Of course, since we are now dealing with random graphs, we consider the distribution of the eigenvalues (mean values and the corresponding variance) obtained with several realizations of the same random graph.

We consider the following random graphs (briefly recalling the definition and some properties).

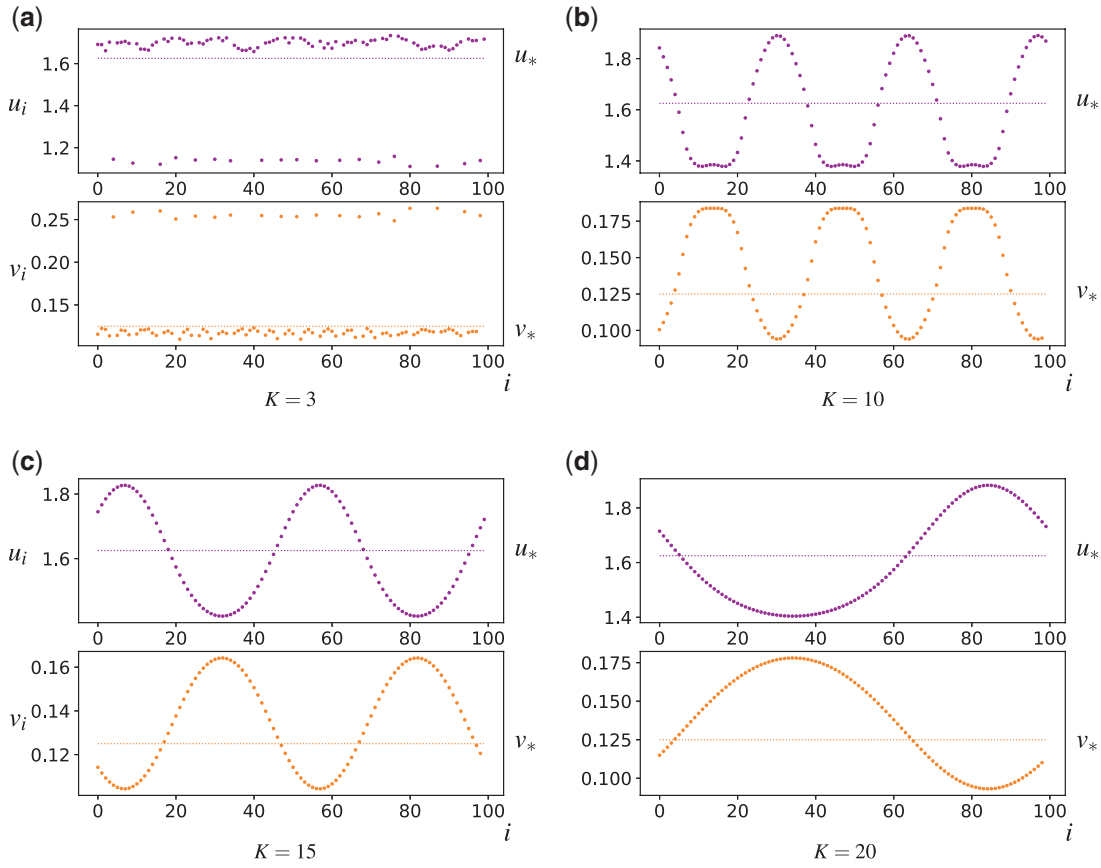

FIG. 3. Steady-state solution for different values of K on a $2K$-regular ring of $N = 100$ nodes and parameter set as in equation (3.7). Initial conditions are random perturbations of the homogeneous state. Identifying each node via its index $i \in \{1, 2, \ldots, N\}$, different kinds of patterns appear.

- *Regular-random graph*
  A random-regular graph is chosen uniformly from the set of all K-regular graphs with N nodes.
- *small-world graph (Watts–Strogatz)* [50] Starting with a regular ring of N nodes in which every node has degree K, each of the edges, in turn, is rewired with some probability p, namely removed and replaced with one that joins two nodes chosen uniformly at random. When $p = 0$, we still have the initial K-regular ring, while with $p = 1$ we obtain a random graph. In the small-world region corresponding to values $10^{-4} < p < 10^{-1}$, the resulting networks are characterized by a small average path length and a large clustering coefficient.
- *binomial graph (Erdős–Réyni)* [51] Considering N nodes, each of the possible edges is chosen with probability p.
- *preferential attachment model (Barabási–Albert)* [52] A graph of N nodes is grown by attaching new nodes each with K edges that are preferentially attached to existing nodes with a high degree.

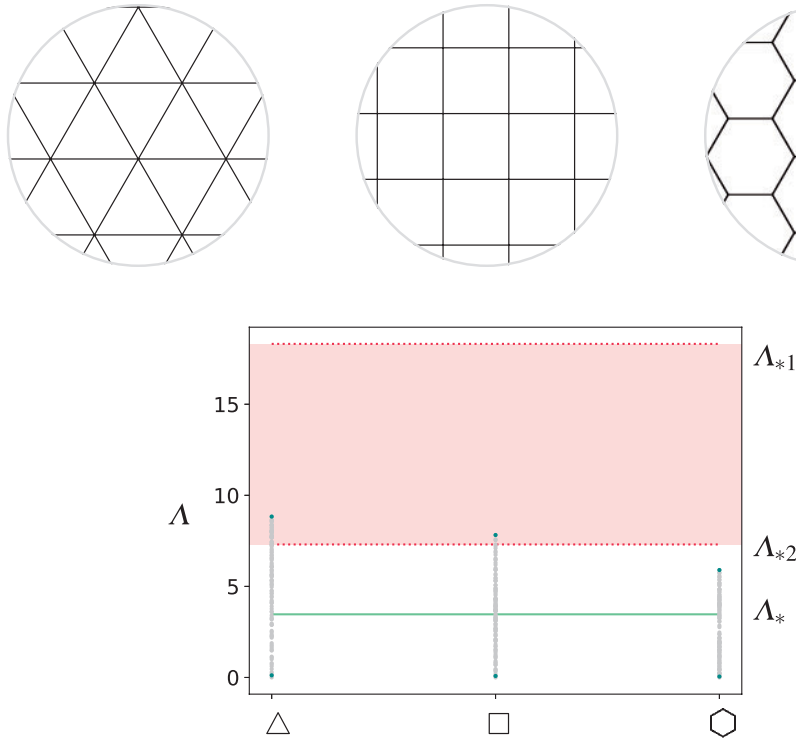

FIG. 4. Cross-diffusion driven instability on triangular (△), square (□) and hexagonal (⬡) lattices (with $N = 110$). Grey dots mark the eigenvalues of the Graph Laplacian, while green dots highlight the smallest and the largest non-zero eigenvalues. Horizontal lines denote the values Λ_{*1}, Λ_{*2} from equation (3.6) (red dotted) and Λ_* (green solid), and the instability region $\Omega_* = (\Lambda_{*1}, \Lambda_{*2})$ is marked with the red stripe (values relevant to the parameter set in equation (3.7) and $d = 0.03$). For interpretation of the color references, the reader is referred to the web version of this article.

We compare these different graph topologies and the appearance of cross-diffusion-induced instability. As in the previous sections, we are interested in the spectrum of the graph Laplacian. Since we deal with particular classes of random graphs, general results cannot be achieved by just looking at a particular realization. For each type of structure, we fix the number of nodes $N = 100$ varying the other network parameters (the probability p for Watts–Strogatz and Erdős–Réyni graphs, the number of edges of a node for random-regular and Barabási–Albert graphs). In Fig. 6, the location of the spectra of these topologies with respect to the instability region (obtained using the parameter set in equation (3.7)) is shown. We generate 1000 realizations of each type of random graphs and each parameter value, obtaining a distribution of the eigenvalues. Grey dots mark the mean of the eigenvalues of the Graph Laplacian, while green dots and error bars highlight the mean and variance of the smallest and the largest non-zero eigenvalues. As for the previous cases, horizontal lines denote the values Λ_{*1}, Λ_{*2} from equation (3.6) (red dotted) and Λ_* (green solid), and the instability region $\Omega_* = (\Lambda_{*1}, \Lambda_{*2})$ is marked with the red stripe.

In a regular-random graph it can be seen that the cross-diffusion induced instability appears on average in the region when $2 \leq K/2 \leq 13$ and $N = 100$, while greater values of the node-degree only lead to a very small probability of instability and the homogeneous steady state is expected to be stable. In a small-world network, with $K/2 = 15$ being fixed, we report in Fig. 6b the averages and variances of

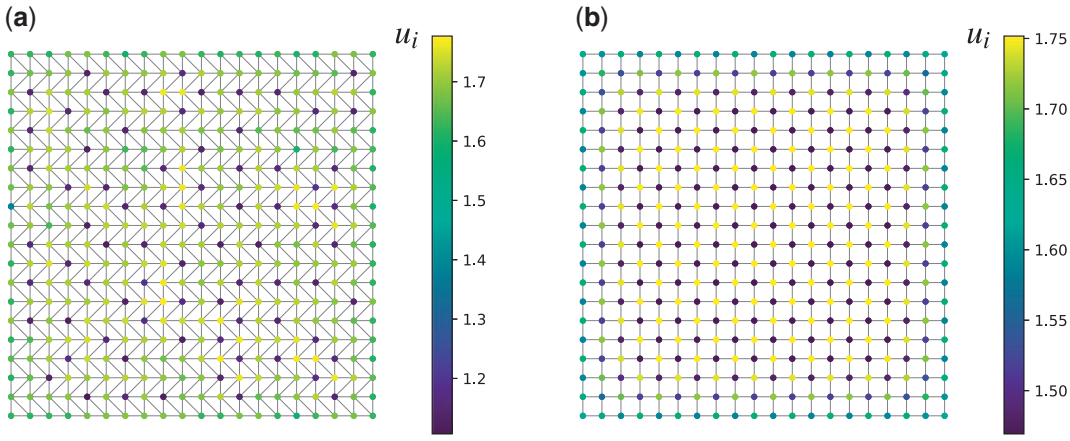

FIG. 5. Steady state (u variable) on a triangular and square lattices with $N = 400$ nodes. The parameter set is reported in equation (3.7) and setting $d = 0.03$. Initial conditions are random perturbations of the homogeneous state. Different colours denote different values of the state variable u and each node in the networks is coloured accordingly to the final steady state. (a) Triangular and (b) square. For interpretation of the color references, the reader is referred to the web version of this article.

the eigenvalues for different values of the probability p of rewiring an edge in a larger interval than the small-world regime. It turns out that the systems show, with a probability well bounded away from zero, non-homogeneous steady states for the considered values of p because at least one averaged eigenvalue is always located well within the instability region. Depending on the number of eigenvalues in the instability region, different types of stable patterns can be observed. For the Erdős–Rényi graph, cross-diffusion induced instability is most likely to appear for small values of the probability p of choosing an edge, while it is not likely to occur for larger values. In order to better compare this structure with the other types, we consider $p \approx 4K/(N-1)$, which for large N approximates the average number of links for one node. With $N = 100$ and $K = 30$, we obtain $p \approx 0.3$, for which the systems display cross-diffusion induced instability with a probability well bounded away from zero. Finally, the Barabási–Albert graph is quite different from the others. The spectrum has a large variance, and especially for large values of K (that in this case represents the number of edges chosen for every new node in the growing process). We observe that the possibility of pattern formation really depends much more on the particular realization of the graph in comparison to the other graph structures.

A final observation has to be made on the non-homogeneous steady state that arises through cross-diffusion induced instability. Its shape is still quite regular and 'smooth' as reported for regular rings in the previous section, but small variations from this regular configuration appear (see Fig. 7). For the other structures instead, the system tends to a stable non-homogeneous configuration that however does not present the characteristic shape of valleys and bumps.

In addition to the phenomenological discussion, ecological back-interpretation is also important. The first crucial observation is that cross-diffusion enables the coexistence of the species with a non-homogeneous distribution. In fact, without cross-diffusion, the homogeneous distribution of the populations (namely all nodes reach the same steady state) is the only outcome. This fact is indeed important in ecology: homogeneity and synchronization of metacommunities may be harmful to species' survival. Cross-diffusion also affects the populations' abundance as observed in the PDEs model. Looking at the total abundance of the species on the network for the simulations presented in the articles and the parameter set considered, we observe a small decrease in the total abundance of population u and an

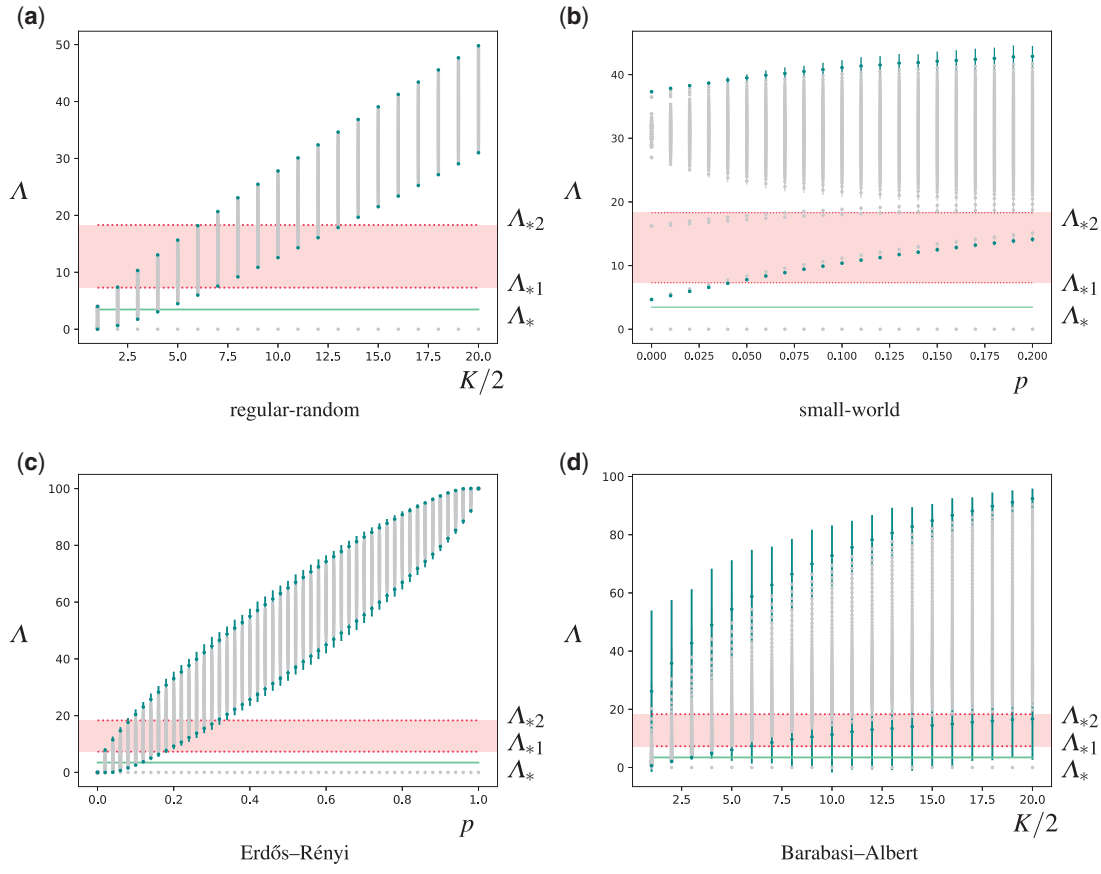

FIG. 6. Comparison of different graph topologies and the appearance of cross-diffusion induced instability. Grey dots mark the eigenvalues of the Graph Laplacian, while green dots and error bars highlight the mean and variance of the smallest and the largest non-zero eigenvalues, obtained with 1000 realization of the random graphs. Horizontal lines denote the values Λ_{*1}, Λ_{*2} from equation (3.6) (red dotted) and Λ_* (green solid), and the instability region $\Omega_* = (\Lambda_{*1}, \Lambda_{*2})$ is marked with the red stripe (values relevant to the parameter set in equation (3.7) and $d = 0.03$). For interpretation of the color references, the reader is referred to the web version of this article.

increase in the total abundance of population v with respect to the homogeneous case (without cross-diffusion). For instance, for the ring topology ($N = 100$, $K = 10$), parameter set as in equation (3.7) and $d = 0.03$, species u decreases of 1.78% while species v increases of 12.3%. This quantitative difference reflects the difference in the order of magnitude of the population sizes at the homogeneous steady state (see for instance Fig. 3) and it is a limitation of the particular parameter set. However, the qualitative trend highlights a counter-intuitive effect driven by cross-diffusion, namely that although species u tries to avoid v, it is actually v that benefits from this. However, it is worthwhile to say that the total population abundance is not the only factor measuring the advantages/disadvantages of the two competing populations.

4. Conclusion and Outlook

In this article, we have investigated the cross-diffusion induced instability, already known in reaction–cross-diffusion systems of PDEs, in networks of dynamical systems. The cross-diffusion terms are

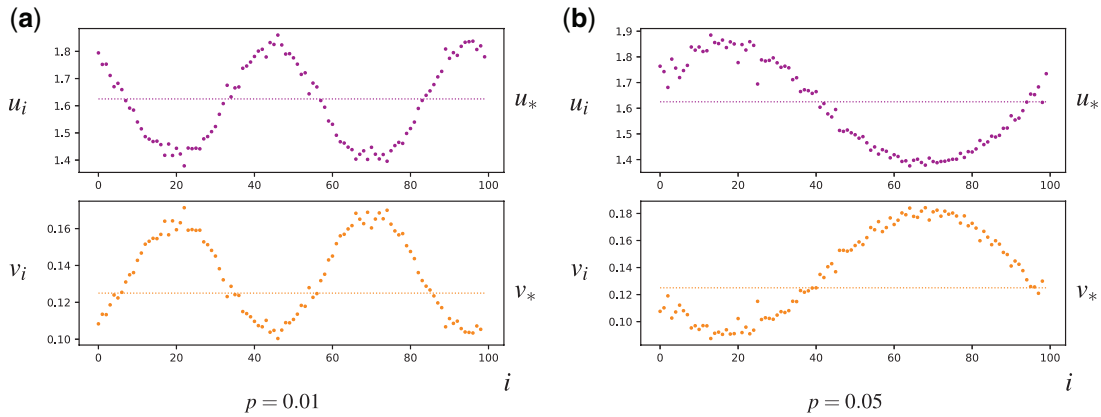

FIG. 7. Non-homogeneous steady state on a small-world network with $N = 100$ and $K = 30$ for different values of the probability p. The parameter set is reported in equation (3.7) and $d = 0.03$. Initial conditions are random perturbations of the homogeneous state.

non-linear and also written using the graph Laplacian, as the standard diffusive coupling. We established the general framework, and we have shown that in this case the linearization slightly differs from the standard case and the PDEs case. Then, we adapted and investigated the SKT cross-diffusion model for competing species on a network. As already known in the context of reaction–cross-diffusion models, the cross-diffusion terms can destabilize the homogeneous equilibrium state and cause the appearance of organized states and patterns, which is not possible only with standard diffusion terms. The important finding is that the obtained conditions for cross-diffusion induced instability in the network framework are the same as the continuous case, where the role of the eigenvalues of the Laplace operator is played by the eigenvalues of the graph Laplacian. Also in this case, an instability region, which depends on the model parameter, characterizes the possibility of observing patterns, understood as non-homogeneous states on the nodes of the network, and the location of the eigenvalues of the graph Laplacian determines their presence and shape. Finally, we have analysed different network structures (such as regular rings, two-dimensional lattices and different random graphs) in order to show how the network structure influences the possible outcomes of the system. In particular, we have looked at the spectrum of the graph Laplacian (or its distribution for random graphs). We conclude that cross-diffusion induced instability depends on the network structure: for instance, for the SKT network model in the weak competition case it is more likely to appear on triangular lattices, and on small-world and Barabasi–Albert random graphs.

One key aim of this work is to point out that non-linear cross-diffusion terms can be a useful tool to model complex systems, and that they can give rise to richer dynamics than with just standard diffusion coupling. In particular, as in the PDEs setting, these non-linear cross-diffusion terms might be derived (at least formally) by a fast-reaction limit. Several research directions arise at this point. On the one hand, we can look at the dynamical and bifurcation aspects of this topic. As widely investigated for cross-diffusion PDEs systems, we want to find an entropy functional or a Lyapunov function for networks in order to achieve global stability results [53–55]. Furthermore, a deeper investigation of the system outcomes combined with the bifurcation structure (that can be computed by the continuation software `pde2path` [56]) may reveal the presence of periodic patterns, as in the PDEs case. On the other hand, one could take an even more detailed look at the influence of the graph topology. In this regard, the parallel between continuous and discrete models is intriguing. Inspired by the discretized version of

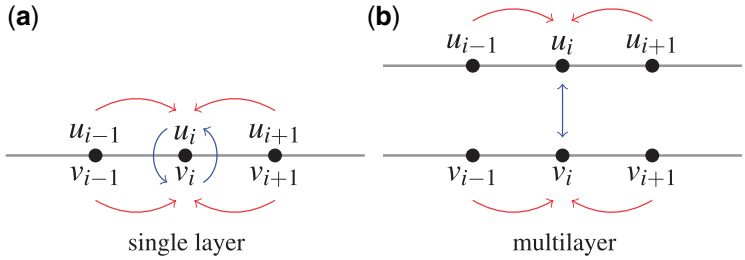

FIG. 8. Different way to model the dynamics of two species on a network: the species evolve, compete and move (a) on the same network or (b) on a multilayer network.

the PDEs model involving the Laplace operator, we considered in this article different graph topologies, changing completely the *corresponding* operator in the continuous case. Therefore, it would be interesting to understand the limit model back to the continuous case. Moreover, following [3], it seems possible to extend the analysis to directed networks and, considering for instance the SKT model on networks, it can also be possible to consider the dynamics of the two competing species evolving on different networks, as sketched in Fig. 8. This would lead us to consider the dynamics on a multilayer network [6, 57, 58], where the two layers can be different, for which the extension of the theory of Turing patterns has already been presented in [5–7]. It could also be interesting to study other types of cross-diffusion terms involving different nodes: for instance, in the SKT model, the movement of one species from node i to node j is influenced by the presence of the same species or the competing one on node j. In this scenario, there is an information flow or knowledge about the status of the other nodes, or it can be seen as a weighted network with link weights depending on the quantities on each node. Finally, one could study possible applications of cross-diffusion systems on networks, ranging from ecology and landscape modelling to disease spreading [42, 59], that are characterized by a strong interplay between dynamics and network structure.

Acknowledgements

The authors thank Esther Daus for the fruitful discussion about the topic of the article.

Funding

C.K. has been supported by a Lichtenberg Professorship of the VolkswagenStiftung. C.K. also acknowledges partial support of the EU within the TiPES project funded by the European Union's Horizon 2020 research and innovation programme under Grant Agreement No. 820970. C.S. has received funding from the European Union's Horizon 2020 research and innovation programme under the Marie Skłodowska–Curie Grant Agreement No. 754462. C.S. also acknowledge the support of IGSSE within the SEND project under Project Teams (14th Cohort) and of the University of Graz through the NAWI Graz Visiting Award 2022 IMSC Young Investigator Fellowship. C.S. is a member of the INdAM-GNFM Group.

REFERENCES

1. TURING, A. (1952) The chemical basis of morphogenesis. *Philos. Trans. R. Soc. B:*, **237**, 37–72.
2. OTHMER, H. & SCRIVEN, L. (1971) Instability and dynamic pattern in cellular networks. *J. Theor. Biol.*, **32**, 507–537.

3. Asllani, M., Challenger, J., Pavone, F., Sacconi, L. & Fanelli, D. (2014) The theory of pattern formation on directed networks. *Nat. Commun.*, **5**, 4517.

4. Nakao, H. & Mikhailov, A. (2010) Turing patterns in network-organized activator–inhibitor systems. *Nat. Phys.*, **6**, 544–550.

5. Asllani, M., Busiello, D., Carletti, T., Fanelli, D. & Planchon, G. (2014) Turing patterns in multiplex networks. *Phys. Rev. E*, **90**, 042814.

6. Brechtel, A., Gramlich, P., Ritterskamp, D., Drossel, B. & Gross, T. (2018) Master stability functions reveal diffusion-driven pattern formation in networks. *Phys. Rev. E*, **97**, 032307.

7. Kouvaris, N., Hata, S. & Díaz-Guilera, A. (2015) Pattern formation in multiplex networks. *Sci. Rep.*, **5**, 1–9.

8. Petit, J., Lauwens, B., Fanelli, D. & Carletti, T. (2017) Theory of Turing patterns on time varying networks. *Phys. Rev. Lett.*, **119**, 148301.

9. Asslani, M., Di Patti, F. & Fanelli, D. (2012) Stochastic Turing patterns on a network. *Phys. Rev. E*, **86**, 046105.

10. Bramburger, J. & Holzer, M. (2023) Pattern formation in random networks using graphons. *SIAM J. Math. Anal.*, **55**, 2150–2185.

11. Anderson Jr, W. & Morley, T. (1985) Eigenvalues of the Laplacian of a graph. *Linear Multilinear Algebra*, **18**, 141–145.

12. Chung, FRK. *Spectral graph theory.* In CBMS Regional Conference Series in Mathematics, Vol. 92, American Mathematical Society, Providence, 1997.

13. Jost, J., Mulas, R. & Münch, F. (2022) Spectral gap of the largest eigenvalue of the normalized graph Laplacian. *Commun. Math. Stat.*, **10**, 371–381.

14. Li, J.-S. & Zhang, X.-D. (1998) On the Laplacian eigenvalues of a graph. *Linear Algebra Appl.*, **285**, 305–307.

15. Merris, R. (1998) A note on Laplacian graph eigenvalues. *Linear Algebra Appl.*, **285**, 33–35.

16. Mohar, B., Alavi, Y., Chartrand, G. & Oellermann, O. (1991) The Laplacian spectrum of graphs. *Graph Theory, Combin. Appl.*, **2**, 12.

17. Dorogovtsev, S., Goltsev, A., Mendes, J. & Samukhin, A. (2003) Spectra of complex networks. *Phys. Rev. E*, **68**, 046109.

18. Chung, F., Lu, L. & Vu, V. (2004) The spectra of random graphs with given expected degrees. *Internet Math.*, **1**, 257–275.

19. Chung, F. & Radcliffe, M. (2011) On the spectra of general random graphs. *Electron. J. Combin.*, **18**, 215.

20. Othmer, H. & Scriven, L. (1974) Non-linear aspects of dynamic pattern in cellular networks. *J. Theor. Biol.*, **43**, 83–112.

21. Segel, L. & Levin, S. (1976) Application of non-linear stability theory to the study of the effects of diffusion on predator-prey interactions. *AIP Conf. Proc.*, **27**, 123.

22. Bonacini, E., Burioni, R., Di Volo, M., Groppi, M., Soresina, C. & Vezzani, A. (2016) How single node dynamics enhances synchronization in neural networks with electrical coupling. *Chaos, Solitons Fractals*, **85**, 32–43.

23. Mulas, R., Kuehn, C. & Jost, J. (2020) Coupled dynamics on hypergraphs: master stability of steady states and synchronization. *Phys. Rev. E*, **101**, 062313.

24. Pecora, L. & Carroll, T. (1998) Master stability functions for synchronized coupled systems. *Phys. Rev. Lett.*, **80**, 2109–2112.

25. Sun, J., Bollt, E. & Nishikawa, T. (2009) Master stability functions for coupled nearly identical dynamical systems. *EPL (Europhys. Lett.)*, **85**, 60011.

26. Bick, C., Böhle, T. & Kuehn, C. (2022) Multi-population phase oscillator networks with higher-order interactions. *Nonlinear Differ. Equ. Appl.*, **29**, 64.

27. Bonetto, R. & Kojakhmetov, H.J. (2022) Nonlinear Laplacian dynamics: symmetries, perturbations, and consensus. arXiv preprint arXiv:2206.04442 (2022).

28. Gambuzza, L., Di Patti, F., Gallo, L., Lepri, S., Romance, M., Criado, R., Frasca, M., Latora, V. & Boccaletti, S. (2021) Stability of synchronization in simplicial complexes. *Nat. Commun.*, **12**, 1255.

29. Mancastroppa, M., Iacopini, I., Petri, G. & Barrat, A. (2023) Hyper-cores promote localization and efficient seeding in higher-order processes. *arXiv, arXiv:2301.04235, preprint: not peer reviewed*.
30. Gierer, A. & Meinhardt, H. (1972) A theory of biological pattern formation. *Kybernetik*, **12**, 30–39.
31. Shigesada, N., Kawasaki, K. & Teramoto, E. (1979) Spatial segregation of interacting species. *J. Theor. Biol.*, **79**, 83–99.
32. Ottaviano, S., Sensi, M. & Sottile, S. (2022) Global stability of SAIRS epidemic models. *Nonlinear Anal.: Real World Appl.*, **65**, 103501.
33. Breden, M., Kuehn, C. & Soresina, C. (2021) On the influence of cross-diffusion in pattern formation. *J. Comput. Dyn.*, **8**, 213.
34. Conforto, F., Desvillettes, L. & Soresina, C. (2018) About reaction–diffusion systems involving the Holling-type II and the Beddington–DeAngelis functional responses for predator–prey models. *Nonlinear Differ. Equ. Appl.*, **25**, 24.
35. Desvillettes, L. & Soresina, C. (2019) Non-triangular cross-diffusion systems with predator–prey reaction terms. *Ricerche di Matematica*, **68**, 295–314.
36. Gambino, G., Lombardo, M. & Sammartino, M. (2008) Cross-diffusion driven instability for a Lotka-Volterra competitive reaction–diffusion system. *Waves and Stability in Continuous Media* (N. Manganaro, R. Monaco & S. Rionero eds). *Proceedings of the 14th Conference on WASCOM 2007*, World Scientific, pp. 297–302.
37. Kuehn, C. & Soresina, C. (2020) Numerical continuation for a fast-reaction system and its cross-diffusion limit. *Partial Differ. Equ. Appl.*, **1**, 1–26.
38. Lacitignola, D., Bozzini, B., Peipmann, R. & Sgura, I. (2018) Cross-diffusion effects on a morphochemical model for electrodeposition. *Appl. Math. Model.*, **57**, 492–513.
39. Soresina, C. (2022) Hopf bifurcations in the full SKT model and where to find them. *Discrete Cont. Dyn. Syst.-S.*, 15.9.
40. Tang, X. & Song, Y. (2015) Cross-diffusion induced spatiotemporal patterns in a predator–prey model with herd behaviour. *Nonlinear Anal.: Real World Appl.*, **24**, 36–49.
41. Daus, E., Desvillettes, L. & Dietert, H. (2019) About the entropic structure of detailed balanced multi-species cross-diffusion equations. *J. Differ. Equ.*, **266**, 3861–3882.
42. Duan, M., Chang, L. & Jin, Z. (2019) Turing patterns of an SI epidemic model with cross-diffusion on complex networks. *Physica A*, **533**, 122023.
43. Yi, F. (2021) Turing instability of the periodic solutions for reaction-diffusion systems with cross-diffusion and the patch model with cross-diffusion-like coupling. *J. Differ. Equ.*, **281**, 379–410.
44. Zheng, Q., Wang, Z. & Shen, J. (2017) Pattern dynamics of network-organized system with cross-diffusion. *Chin. Phys. B*, **26**, 020501.
45. Slavík, A. (2020) Lotka–Volterra competition model on graphs. *SIAM J. Appl. Dyn. Syst.*, **19**, 725–762.
46. Kuehn, C. & Soresina, C. (2023) Supplementary material. Matlab scripts https://github.com/soresina/SKT_on_networks. Accessed April 24, 2023.
47. Python Software Foundation (2020) Python Language Reference (version 3.8.3).
48. Hagberg, A., Schult, D. & Swart, P. (2008) Exploring network structure, dynamics, and function using NetworkX. *Proceedings of the 7th Python in Science Conference (SciPy2008)* (G. Varoquaux, J. Millman, & T. Vaught eds). pp. 11–15. https://conference.scipy.org/proceedings/scipy2008/.
49. Wu, J., Barahona, M., Tan, Y.-J. & Deng, H.-Z. (2011) Robustness of regular ring lattices based on natural connectivity. *Int. J. Syst. Sci.*, **42**, 1085–1092.
50. Watts, D. & Strogatz, S. (1998) Collective dynamics of 'small-world' networks. *Nature*, **393**, 440–442.
51. Erdős, P. & Rényi, A. (1960) On the evolution of random graphs. *Publ. Math. Inst. Hung. Acad. Sci.*, **5**, 17–60.
52. Barabási, A.-L. & Albert, R. (1999) Emergence of scaling in random networks. *Science*, **286**, 509–512.
53. Belykh, V., Belykh, I. & Hasler, M. (2004) Connection graph stability method for synchronized coupled chaotic systems. *Physica D*, **195**, 159–187.
54. Li, M. & Shuai, Z. (2010) Global-stability problem for coupled systems of differential equations on networks. *J. Differ. Equ.*, **248**, 1–20.

55. Slavík, A. (2021) Reaction–diffusion equations on graphs: stationary states and Lyapunov functions. *Nonlinearity*, **34**, 1854.
56. Uecker, H. (2021) `pde2path` without finite elements. https://www.staff.uni-oldenburg.de/hannes.uecker/pde2path/tuts/modtut.pdf.
57. Aleta, A. & Moreno, Y. (2019) Multilayer networks in a nutshell. *Annu. Rev. Condens. Matter Phys.*, **10**, 45–62.
58. Kivelä, M., Arenas, A., Barthelemy, M., Gleeson, J., Moreno, Y. & Porter, M. (2014) Multilayer networks. *J. Complex Netw.*, **2**, 203–271.
59. Lang, J., De Sterck, H., Kaiser, J. & Miller, J. (2018) Analytic models for SIR disease spread on random spatial networks. *J. Complex Netw.*, **6**, 948–970.

A. Derivation of the SKT model on networks

As for the SKT model in the PDEs setting, the particular expression of the cross-diffusion terms can be justified (at least formally) also for the SKT model on networks exploiting different time scales.

To this end, we consider two possible states of the individual of the population u on each node, namely quiet and scared individuals, denoted by u_{Ai} and u_{Bi}, $i = 1, \dots, N$, respectively. Then, the total population u on each node is given by $u_i = u_{Ai} + u_{Bi}$, $i = 1, \dots, N$. Moreover, we model the movements from one node to the others using the standard diffusive coupling and assuming that scared individuals have a larger diffusion coefficient than quiet individuals d_A. The transition from the quiet to the scared state and vice-versa depends on the competing species v and it happens on a faster time scale (denoted by ε). The system of equations for the network dynamics is given by

$$\begin{cases} \dot{u}_{Ai} = (r_1 - a_1 u_i - b_1 v_i) u_{Ai} - d_A \displaystyle\sum_{j=1}^{N} l_{ij} u_{Aj} + \frac{1}{\varepsilon}\left(u_{Bi}\left(1 - \frac{v_i}{M}\right) - u_{Ai}\frac{v_i}{M}\right), \\ \dot{u}_{Bi} = (r_1 - a_1 u_i - b_1 v_i) u_{Bi} - (d_A + \hat{d}M) \displaystyle\sum_{j=1}^{N} l_{ij} u_{Bj} - \frac{1}{\varepsilon}\left(u_{Bi}\left(1 - \frac{v_i}{M}\right) - u_{Ai}\frac{v_i}{M}\right), \\ \dot{v}_i = (r_2 - b_2 u_i - a_2 v_i) v_i - d \displaystyle\sum_{j=1}^{N} l_{ij} v_j. \\ i = 1, \dots, N, \end{cases} \tag{A.1}$$

where $M \geq r_2/b_2$ is a constant needed to ensure that the transition rate from the scared to the excited state is positive.

When the transition from one state to the other is much faster than the competition process, namely $\varepsilon \to 0$, we expect

$$u_{Bi}\left(1 - \frac{v_i}{M}\right) - u_{Ai}\frac{v_i}{M} = 0 \quad i = 1, \dots, N.$$

Together with $u_i = u_{Ai} + u_{Bi}\, i = 1, \dots, N$, one can obtain u_{Ai} and u_{Bi} as function of u_i and v_i. Moreover, by adding the equation for u_{Ai} and u_{Bi} allows us to reduce system (A.1) to a two-species system on each node. The limiting system corresponds (at least formally) to system (3.3) with only the non-linear cross-diffusion term in the equations for the state variables u_i (namely $D_{21} = 0$).

Therefore, from the modelling perspective, the non-linear cross-diffusion term naturally incorporates processes occurring at different time scales. In particular, the avoidance mechanism of species u versus species v described by the dichotomy of quiet/excited is encapsulated in the cross-diffusion term.